HHS Public Access

Author manuscript

Addict Biol. Author manuscript; available in PMC 2024 March 09.

Published in final edited form as:

Addict Biol. 2023 August ; 28(8): e13286. doi:10.1111/adb.13286.

Δ^9-tetrahydrocannabinol self-administration induces cell-type specific adaptations in the nucleus accumbens core

Constanza Garcia-Keller[1,3,*], **Madeline Hohmeister**[1,*], **Kailyn Seidling**[1,*], **Lauren Beloate**[1], **Vivian Chioma**[1], **Sade Spencer**[2], **Peter Kalivas**[1,#], **Daniela Neuhofer**[1,#]

[1]Department of Neurosciences, Medical University of South Carolina, 173 Ashley Avenue, BSB 403-MSC 510, Charleston, SC 29425.

[2]Department of Pharmacology, Medical Discovery Team on Addiction, University of Minnesota, Minneapolis, Minnesota, MN 55455.

[3]Department of Pharmacology and Toxicology, Medical College of Wisconsin, 8701 W Watertown Plank Road, Milwaukee, WI 53226.

Abstract

Drugs of abuse induce cell type specific adaptations in D1- and D2-medium spiny neurons (MSNs) in the nucleus accumbens core (NAcore), that can bias signaling towards D1-MSNs and enhance relapse vulnerability. Whether Δ^9-tetrahydrocannabinol (THC) use initiates similar neuroadaptations is unknown. D1- and D2-Cre transgenic rats were transfected with Cre-dependent reporters and trained to self-administer THC+cannabidiol (THC+CBD). After extinction training spine morphology, glutamate transmission, CB1R function and cFOS expression were quantified. We found that extinction from THC+CBD induced a loss of large spine heads in D1- but not D2-MSNs and commensurate reductions in glutamate synaptic transmission. Also, presynaptic CB1R function was impaired selectively at glutamatergic synapses on D1-MSNs, which augmented the capacity to potentiate glutamate transmission. Using cFOS expression as an activity marker, we found no change after extinction but increased cFOS expression in D1-MSNs after cue-induced drug-seeking. Contrasting D1-MSNs, CB1R function and glutamate synaptic transmission on D2-MSN synapses were unaffected by THC+CBD use. However, cFOS expression was decreased in D2-MSNs of THC+CBD-extinguished rats and was restored after drug-seeking. Thus, CB1R adaptations in D1-MSNs partially predicted neuronal activity changes, posing pathway specific modulation of eCB signaling in D1-MSNs as a potential treatment avenue for cannabis use disorder (CUD).

Keywords

Addiction; Cannabinoid Receptor 1; Δ^9-tetrahydrocannabinol; Medium spiny Neurons; Nucleus Accumbens; Synaptic Plasticity

Correspondence: Daniela Neuhofer, Medical University of South Carolina, 173 Ashley Avenue, BSB 403-MSC 510, Charleston, SC 29425. neu.dani@gmx.at.

*Shared equally as first authors

#Shared equally as senior authors

Conflict of Interest

The authors report no biomedical financial interests or potential conflicts of interest.

Introduction

Cannabis is rapidly being legalized around the globe with more than 190 million users [1]. Approximately 30% of chronic users will develop cannabis use disorder (CUD)[2], which is characterized by escalating use, failure to quit, craving, negative affect and high risk for relapse[3].

Δ^9-tetrahydrocannabinol (THC) is the major psychoactive component of cannabis and a partial agonist at the cannabinoid receptor 1 (CB1R)[4]. The activation of presynaptic CB1R inhibits neurotransmitter release, and can induce presynaptic long-term depression (LTD)[5]. Chronic THC exposure causes functional tolerance of CB1R in the striatum and nucleus accumbens[6–9]. Chronic THC also induces adaptations beyond CB1 and the endocannabinoid system[3], including adaptations at glutamatergic synapses in the prefrontal cortex (PFC) [10] and nucleus accumbens (NAc)[9,11].

The NAc core (NAcore) is an essential component of the mesocorticolimbic system and important for motivation and reward[12]. Accumbens adaptations that disrupt glutamate homeostasis drive drug seeking after the chronic use of cocaine, nicotine and heroin[13,14]. GABAergic D1- and D2-medium spiny neurons (MSNs) together comprise 90–95% of all neurons in the NAcore[15] and express D1 or D2 dopamine receptors, respectively. Studies using cell type specific expression of activity indicators such as cfos immunoreactivity or cell selective opto- or chemogenetic stimulation in the NAc demonstrate that D1-MSNs promote and D2-MSNs inhibit certain reward behaviors[16,17]. Distinct MSN-type specific adaptations after chronic cocaine and morphine have been described that bias towards D1-MSN signaling after drug exposure[17–20]. We previously employed an intravenous self-administration (SA) model of THC in combination with another phytocannabinoid cannabidiol (CBD) to show that animals reliably self-administer THC+CBD and reinstate to drug associated cues[9,11]. While only THC is psychoactive, CBD decreases the anxiogenic effects of THC[21] and increases lever discrimination during self-administration[22]. THC+CBD SA caused loss of spine density and desensitization of CB1R that caused loss of long term synaptic plasticity in NAcore MSNs[9,11]. Here we investigate whether these THC+CBD induced NAcore neuroadaptations are cell-type specific and drive changes in neuronal activity. To address these questions, D1- and D2-Cre transgenic rats were transfected with Cre-dependent reporters, underwent THC+CBD SA and were evaluated for changes in D1- and D2-MSN specific morphology, CB1 function, glutamatergic transmission, glutamatergic plasticity and cFOS expression as a proximate marker of cellular activity. We discovered a reduction in basal glutamate transmission and desensitization of CB1R in the NAcore, that was selective for glutamatergic synapses onto D1-MSNs. The D1-MSN specific neuroadaptations were paralleled by an increased cFOS expression during cue-induced reinstatement. Despite the lack of significant adaptations on glutamatergic synapses onto D2-MSNS, our measures of cFOS expression indicated that D2-MSN hypoactivity 24h after the last extinction session was partially restored during cue-induced reinstatement. Our results suggest that hypoactivity of D2-MSNs during withdrawal and hyperactivity of D1-MSNs during reinstatement are biomarkers of withdrawal from Cannabis use that are shared with other drugs of abuse.

Methods

Catheter Surgery:

LE-Tg(Drd1a-iCre)3Ottc and LE-Tg(Drd2-iCre)1Ottc rats (cre recombinase under control of the dopamine receptor D1 or D2 promoter) were kindly provided by NIDA and previously validated[23]. Males and females rats were bred at our animal facility, kept in a 12–12 hour reverse light-dark cycle and experiments were performed during the dark cycle and catheter surgery performed when rats were ~70 days old. Before surgery, animals were anesthetized with ketamine (100 mg/kg) and xylazine (7 mg/kg), together with ketorolac analgesic (0.28–0.32 mg/kg) and prophylactic antibiotic (Cefazolin, 200 mg/ml, subcutaneous; West-Ward Pharmaceuticals, NJ). Over the course of the project, we switched to isoflurane anesthesia (induction 5%, maintenance 1.5–2.5%). Rats were implanted with indwelling jugular catheters as described previously[11].

A total of 82 out of 97 rats entered the study (THC+CBD SA +Extinction N=35, THC+CBD SA +Extinction+Reinstatement N=25, vehicle SA=22) completed the protocol and were included in data analysis. Seven animals were excluded from the study due to failing catheters or sickness during SA, eight animals were excluded during or after extinction training because of sickness or missed virus placement. Tissue of animals was shared between different patch-clamp experiments, spine morphology and cFOS quantification, (eg, different slices from the same animal were used for WIN-55,212–22 and LFS-plasticity experiment). The number of drug infusions was also similar for the different experiments performed in this study (Figure S1).

Virus injections:

During catheter surgery, AAV2.EF1a.DIO.eYFP.WPRE.hGH (Addgene27056, for patch-clamp experiments) or pAAV.CAG.Flex.Ruby2sm-Flag.WPRE.SV40 (Addgene 98928, for spine analysis) was infused bilaterally into the NAcore (AP +1.5mm, ML ±1.7mm, V-7.2mm) with a rate of (0.75µl of, 0.15 µl/min to induce Cre-dependent expression of the reporter eYFP).

THC+CBD SA, extinction and reinstatement:

Rats had one week of recovery from surgery before starting behavioral training. The SA procedure has been described in detail elsewhere[11]. Briefly, following 5 days of THC+CBD vapor pre-exposure, animals were food deprived for 24 h, then underwent a 2-hour food training session for 2 days in which presses on the active lever resulted in the delivery of a single food pellet (45 mg, Noyes) on a fixed-ratio 1 (FR1) schedule of reinforcement. Following food training, animals remained food restricted throughout SA. Rats began daily 90 min SA sessions with fixed ratio 1 delivery of intravenous THC+CBD in a 10:1 dose ratio (THC/infusion=60 µg on days 1–5, and THC/infusion=30 µg on all subsequent days), paired with tone and light cues over a 2-week period. THC+CBD (NIDA, Bethesda, MD, USA) was dissolved in vehicle containing 0.28% ethanol, an equivalent concentration of Tween 80, and saline to volume. The vehicle solution for the vehicle control group was made up identically but without THC+CBD. Vehicle rats were exposed to 5 days of vehicle vapor, were food deprived and food trained as described above for the THC+CBD treatment

groups. The rats were then allowed to self-administer the vehicle using the same protocol as the THC+CBD self-administration groups. Following self-administration, the rats underwent extinction training in which lever presses were recorded but did not result in drug infusion or presentation of the drug-paired cues. Tissue was obtained 24hr after the last extinction session or after 30–60 min of cued reinstatement (Figure 1A). The 30 minutes time point was chosen for whole cell patch clamp and spine imaging as it has been previously shown that morphological and physiological synaptic changes are transient and peak at 15–45 min after initiating cocaine reinstatement[24]. The 60 minutes time point was chosen because the cFOS protein expression peaks at this time point[25].

Discrimination between the active and inactive levers was calculated as the discrimination index [(active lever presses – inactive lever presses)/(active lever presses + inactive lever presses) where 0 equals no discrimination and 1 equals complete discrimination].

In vitro whole cell patch clamp recordings:

Fresh NAc slices (250μm; VT1200S Leica vibratome) were collected into a vial containing aCSF as follows (in mM: 126 NaCl, 1.4 NaH2PO4, 25 NaHCO3, 11 glucose, 1.2 MgCl2, 2.4 CaCl2, 2.5 KCl, 2.0 sodium pyruvate, 0.4 ascorbic acid, bubbled with 95% O2 and 5% CO2) and a mixture of 5 mM kynurenic acid and 50 μM D-APV. Slices were kept at 22°C–24°C until they were used for recordings, and were constantly perfused with oxygenated aCSF heated to 32°C (TC-344B, Warner Instruments). GABAA synaptic transmission was blocked with 50μM picrotoxin (Tocris). Neurons were visualized with a Zeiss Axioscope 2 FS plus microscope with a 40x objective and voltage clamp recordings (Multiclamp 700B, Molecular Devices) performed from visualized MSNs in the medial NAc core near the anterior commissure. Glass microelectrodes (1.5–2.5 ΩM) were prepared using a PC-10 vertical puller (Narishige) and filled with internal solution as follows (in mM: 124 cesium methanesulfonate, 10 HEPES potassium, 1 EGTA, 1 MgCl2, 10 NaCl, 2.0 MgATP, and 0.3 NaGTP, 1 QX-314, pH 7.2–7.3, 280 mOsm). To evoke postsynaptic currents, a bipolar stimulating electrode was placed 300μm dorso-medial of the recorded cell. Data was acquired at 10 kHz and filtered at 2 kHz using AxographX software (Axograph Scientific). The stimulation intensity chosen to evoke ~75–50% of maximal AMPA current.

LTD-Protocol:

MSNs were voltage clamped at −80 mV and a stable AMPA baseline response was recorded for at least 10 minutes. For LTD induction, cells were clamped to −50 mV for 3 minutes during which afferents were stimulated at 5 Hz. This sequence was repeated 3X with intermittent 5 min baseline recordings at −80 mV[9,26,27].

Perfusion and tissue preparation:

24hr after the last extinction session or immediately after the 30–60 min reinstatement session, the rats were anesthetized and perfused transcardially. Brains were removed, incubated for 2hr in 4% PFA and coronally sectioned at 100μm on a vibrating-blade microtome (Leica).

Immunohistochemistry and Dendritic Spine Morphology:

We delivered pAAV.CAG.Flex.Ruby2sm-Flag.WPRE.SV40 during catheter surgery to induce Cre-dependent expression of the epitope tag Ruby2sm-Flag, in either D1- or D2-MSNs. Slices were incubated in 3% BSA and 0.03% Triton in PBS for 1hr and incubated in primary antibody 1:500 (rabbit anti-flag, Sigma) diluted in blocking solution overnight at 4°C. Sections were be rinsed and incubated with secondary antibody 1:1000 (goat anti-rabbit Alexa 488, Life Technology), for 3hr at room temperature. After rinsing with 0.1% Triton, tissue was mounted onto glass slides and coverslipped with ProLong Gold antifade (Thermo Fisher)[28]. Labeled sections in the NAcore were imaged using a confocal microscope (Leica SP5, Wetzlar, Germany) (Figure S3A). Images of labeled dendritic segments were acquired via optical sectioning using a 63X oil immersion objective with a numerical aperture of 1.4 using a 3.5x digital zoom. Acquisition settings were as follows: 1024×256 frame size, frame average of 4, and a 0.21 μm z step size. Following acquisition, Z-stacks were exported to BitPlane Autoquant (Media Cybernetics, Rockville, MD) for deconvolution. Only spines on dendrites beginning at >75 μm and ending at ≤200 μm distal to the soma and after the first branch point were quantified (Figure S3B). Individual spines were analyzed using the Imaris software version 8 (Bitplane Inc, Concord, MA) filament module (Figure S3). At least four dendritic segments were analyzed per animal. Spine head diameter was calculated, with the minimum diameter for identification at 0.14 μm. Spine density was normalized to the length of each segment. Treatment groups were unknown to the experimenter.

Immunohistochemistry and cFOS count:

For cFOS experiments the IHC for Flag was combined with IHC for cFOS. Free-floating sections were rinsed in PBS-Triton (0.25%) and incubated in normal goat serum and primary antibodies (mouse anti-flag, Sigma, 1:500, rabbit anti-phospho-cFos, Cell Signaling Technology, 1:1000, MA, USA) overnight at 4°C. After multiple PBS-Triton rinses, sections were incubated in Alexa-Fluor conjugated secondary antibodies (goat anti-mouse Alexa 488 for FLAG, goat anti-rabbit cFOS, Life Technologies, 1:1000) over night. Labeled sections in the NAcore were imaged using a confocal microscope (Zeiss) (Figure 5A+B) with 20x magnification. Acquisition settings were as follows: 299×299 frame size, frame average of 4, and a 0.15 μm z step size. Following acquisition, 15 μm thick Z-stacks were exported to BitPlane Autoquant (Media Cybernetics, Rockville, MD) for deconvolution. The number of cFOS+ cells, Flag+ cells and overlap between cFOS and Flag were quantified using the Imaris software version 8 (Bitplane Inc, Concord, MA) software by an observer blinded to the group allocations to avoid any biasing effects. Only images with more than 50 Flag positive cells were used for analysis. 4 Images had to be discarded for that reason. 2–5 images were analyzed per animal in the medial NAc Core, sampling Bregma 2.52 to 1.68 (see Figure S5)

Statistics:

All data were analyzed using Prism, version 8.0 (GraphPad Software, La Jolla, CA, USA). A Saphiro-Wilk test for Normality was performed and the subsequent statistical tests were chosen accordingly. T-tests, 1-way, 2-way, 3-way and nested ANOVAs + Holm Sidak's multiple comparisons tests were used for normally distributed data sets. Mann-Whitney test

and Kruskal-Wallis test with Dunn's post-hoc test were used for not normally distributed data sets.

Results

D1 and D2 BAC-transgenic rats display similar THC+CBD SA behavior.

D1 and D2-Cre rats were trained to self-administer THC+CBD and then extinguished. Figure 1A shows the treatment groups used: Vehicle + extinction (Ctrl), THC+CBD + extinction (Ext), THC+CBD + extinction + cued reinstatement (Rst). Figure 1B summarizes the comparable lever presses during THC+CBD acquisition and extinction behavior separated by transgenic lines. 2-way ANOVA revealed significant difference in active vs inactive lever presses during SA and extinction in D1-cre (interaction: $F_{(19,1253)}$=2.88, p<0.001, time: $F_{(1.48,97.66)}$=4.57, p=0.02, levers: $F_{(1,66)}$=24.15, p<0.001) and D2-cre rats (interaction: $F_{(19,948)}$=2.73, p<0.001, time: $F_{(6.74,336.7)}$=4.56, p<0.001, levers: $F_{(1,50)}$=14.98, p<0.001). There were no differences in average daily infusion rate between D1 vs D2-cre rats (Figure 1C, p=0.633 Mann Whitney test). D1 vs D2 Cre rats showed both similar cue-induced reinstatement (Figure 1D; rat strain x test phase $F_{(1,92)}$ =0.025, p=0.875; rat strain x lever F(1,92)=1.163, p=0.284, test phase x lever F(1,92) = 8.814, p=0.005; rat strain x test phase x lever $F_{(1,92)}$ =0.009, p=0.927; 3-way ANOVA; D1 Rst active vs inactive lever p=0.006, D1 Rst active vs Ext active lever p=0.002; D2 Rst active vs inactive lever p=0.09, D2 Rst active vs Ext active p=0.0004, Holm Sidak's multiple comparisons test). We furthermore found no differences in SA behavior or reinstatement between male and female rats (see Figure S1A-D).

In accordance with previous studies[11,29], although THC+CBD and vehicle elicited comparable lever pressing and number of average infusions (22.72 vs 20.81 infusions; Figure S1E, F), However, the significantly lower discrimination index in vehicle controls as compared to animals administering THC+CBD indicates a better discrimination between active and inactive lever for drug self-administering animals (Figure S1G).

The loss of large spine heads and decrease in basal spontaneous glutamate transmission indicated pruning of D1-MSNs, but not D2-MSN synapses after THC+CBD

Previous reports show that chronic THC leads to a loss of spines in the PFC[10] and NAc[11]. To test whether THC+CBD SA differentially affected synapses onto D1- versus D2-MSNs, we made three-dimensional (3D) renderings of confocal images from identified D1-MSNs and D2-MSNs in the NAcore that were Alexa-488 labeled with the epitope tag Ruby2sm-Flag[28]. Figure 2A shows representative D1-MSN dendrite segments for the 3 treatment groups. The average spine head diameter (dh) was decreased in THC+CBD extinguished but not cue-reinstated rats compared to vehicle controls (Figures 2B left panel, ($F_{(2,12)}$=4.56, p=0.034; Ctrl vs. Ext p=0.026, Ctrl vs. Rst p=0.13; Nested one-way ANOVA with Holm Sidak's multiple comparisons test). The average spine density was not different between treatment groups (Figures 2B right panel, ($F_{(2,12)}$=1.20, p=0.33; Nested one-way ANOVA). The dh frequency distribution in Figure 2C demonstrates a shift from bigger to smaller spines after extinction from THC+CBD SA with intermediate changes after cue-induced reinstatement (interaction $F_{(16,520)}$=6.34, p<0.01, frequency $F_{(2.304,149.8)}$=323.9

p<0.01, treatment $F_{(2,65)}$=1.12 p=0.33; 2-way ANOVA with repeated measures over spine head diameter and Holm Sidak's multiple comparisons test).

To determine whether the THC+CBD induced loss of large dendritic spines in D1-MSNs was accompanied by a reduction of functional synapses, slices containing the NAcore were prepared after completing the behavioral procedures and whole-cell patch-clamp recordings made in visualized D1-MSNs. Figure 2D shows representative traces of spontaneous excitatory postsynaptic currents (sEPSCs) D1-MSNs for each treatment group. We found no difference in the average amplitude of spontaneous events (Figure 2E, p=0.858, Kruskal-Wallis test). However, the average inter-event-interval in THC+CBD extinguished rats was significantly increased, and this increase remained after cue-induced reinstatement (Figure 2F, p=0.01, Kruskal-Wallis test, Ctrl vs Ext p=0.03, Ctrl vs RST p=0.02, Dunn's multiple comparison). The paired-pulse ratio (measured using a 50 ms interstimulus interval) was not different between Ctrl (1.12±0.08), THC+CBD extinguished (1.18±0.11) and reinstated (1.06±0.04) rats (p=0.829, Kruskal-Wallis test), supporting that the reduced spontaneous activity is more likely due to a loss of AMPAR containing synapses rather than a decrease in release probability.

Equivalent to Figure 2, we quantified the spine morphology and basal AMPAR transmission in D2-MSNs in Figure 3. Figure 3A shows representative D2-MSN dendrite segments for the 3 treatment groups. The average spine dh and average spine density were not different across the three treatment groups (Figures 3B, spine head: $F_{(2,8)}$ =0.639, p=0.553; spine density: $F_{(2,8)}$ =1.433, p=0.294). However, while the dh frequency distribution (Figure 3C) was not different between Ctrl and Ext animals there was a shift from larger to smaller spines in rats that underwent cued reinstatement (interaction $F_{(16,424)}$=2.09, p<0.01, frequency $F_{(2.710,143.6)}$=176.7 p<0.01, treatment $F_{(2,53)}$=2.13 p=0.13; 2-way ANOVA with repeated measures over spine head diameter). Figure 3D shows representative traces of spontaneous activity from NAcore D2-MSNs for each treatment group. The shift from larger to smaller dendritic spines in reinstated animals was not reflected in changes in sEPSC amplitude (Figure 3E; $F_{(2,36)}$=0.013, p=0.99; 1-way ANOVA) or frequency (Figure 3F; ($F_{(2,36)}$=0.95, p=0.30; 1-way ANOVA).

THC+CBD SA decreases CB1R function and is accompanied by potentiation of D1-MSNs after a low-frequency-pairing protocol

The desensitization of CB1R by chronic THC is region and activity dependen[8]. Hence, we probed if THC+CBD intake induced changes in CB1R function of glutamatergic synapses onto D1-MSN and D2-MSNs. To this goal, whole cell patch-clamp recordings of visualized D1-MSNs from THC+CBD extinguished and vehicle control animals were performed and the inhibition of glutamate transmission after CB1R activation measured. We found that the capacity of the CB1R agonist WIN55,212–22 (5 μM dissolved in 0.5% DMSO and ACSF, Sigma) to inhibit glutamatergic transmission was reduced in NAcore slices from THC + CBD-extinguished animals. (Figure 4A, left graph: time $F_{(2.486,\ 29,84)}$=34.51, p<0.01; treatment $F_{(1,12)}$=3.994, p=0.07, interaction $F_{(19,\ 228)}$=2.52, p<0.01; p=0.07; 2-way ANOVA for time course of current response after WIN55,212–22 application, right graph: p=0.026, Mann-Whitney test).

We recently demonstrated that chronic THC+CBD induced a loss of CB1R function that also resulted in a loss of NMDAR dependent long-term depression (LTD)[9]. Here we examined THC+CBD induced metaplasticity on D1-MSNs synapses using a low-frequency pairing protocol. Although we did not observe NMDAR-LTD in vehicle controls, which might be due to the different rat strains used (see discussion), we found significant differences between the 3 treatment groups. D1-MSNs in slices from THC+CBD extinguished rats exhibited significant long-term potentiation (LTP) (Figure 4B; left graph: reinstatement interaction $F_{(32,528)}$=0.35, p<0.99; time, $F_{(3.859,128.5)}$=12.31, p<0.01; treatment $F_{(2,33)}$=4.12, p=0.02; 2-way ANOVA for time course of current response after plasticity induction; right graph: ($F_{(2,31)}$=5.122, p=0.01 one-way ANOVA, Ctrl vs Ext p=0.01, Ctrl vs Rst=0.626, Holm Sidak's multiple comparison test). Measurements of changes in sEPSC event number indicate a presynaptic locus of the LTP (Figure S4). Surprisingly, D1-MSNs from reinstated animals showed a reversal of the extinction associated LTP and responded similarly to vehicle control animals.

Next we probed the CB1R function of glutamatergic synapses onto D2-MSNs by measuring the inhibition of glutamate transmission with the CB1R agonist WIN55,212–22 (Figure 4C). Contrary to D1-MSN glutamatergic synapses, we found that the ability of WIN55,212–22 to inhibit glutamatergic transmission was not different between THC+CBD extinguished animals and vehicle controls (Figure C, left graph: time $F_{(1.995, 21.94)}$=31.8, p<0.01; treatment $F_{(1,11)}$=0.25, p=0.63; interaction $F_{(18, 198)}$=1.36, p=0.15; 2-way ANOVA for time course of current response after WIN55,212–22 application; right graph: $t_{(11)}$=0.40; p=0.69; unpaired t-test)). Also, in contrast to D1-MSNs, the low frequency pairing protocol did not induce any plasticity in D2-MSNs (Figure 4D; left graph: interaction $F_{(32, 368)}$=0.51, p<0.99, time $F_{(2.219, 51.04)}$=2.46, p=0.09; treatment $F_{(2,23)}$=0.002, p=0.99; 2-way ANOVA for time course of current response after plasticity induction; right graph: $t_{(7)}$=2.92, p<0.05, student's t-test).

cFOS in D2-MSNs was decreased 24h after extinction from THC+CBD and cFOS in D1-MSNs was increased after 1 hour of cue-induced reinstatement.

Next we wanted to test whether the identified D1-MSN specific neuroadaptations were associated with cell type specific changes in neuronal activity by quantifying the expression of cFOS, an immediate early gene used as a marker of neuronal activation (Figure 5A,B)[30]. Counting the total number of cFOS expressing cells in tissue sections of the NAcore, we found an increase of cFOS expression after 30 minutes of cue-induced reinstatement that was further increased after 60 minutes cue-induced reinstatement (Figure 5C, p<0.001, Kruskal Wallis test; Veh vs. Rst 60 mins p<0.0001, Ext vs. Rst 30 mins p=0.019, Ext vs. Rst 60 mins p=0.005; Dunn's post-hoc test). Next we looked at the overlap of cells expressing the cre-dependent marker with cells that expressed cFOS. Figures 5D+E summarize the percentage of Flag positive cells that also express cFOS. In contrast to the adaptations that we found in glutamate transmission for this cell population after extinction from THC+CBD, the percentage of D1-MSNs neurons expressing cFos was not altered by extinction from THC+CBD. After 30 minutes of cue-induced reinstatement the overlap was still indistinguishable from the vehicle and extinguished group, although there was a trend towards an increase in cFos expression in D1-MSNs after 60 minutes reinstatement

(Figure 5D; $F_{(3,13)}$=3.44, p=0.05, Nested one-way ANOVA; Veh vs Ext p=0.4494, Veh vs Rst 60 min p=0.084, Ext vs Rst 60 min, p=0.058, Holm-Sidak's multi-comparison test). Interestingly, the percentage of D2-MSNs expressing cFOS was significantly decreased after extinction from THC+CBD and this change in activity was partly restored by 30 and 60 minutes cue-induced reinstatement (Figure 5E, $F_{(3,10)}$=3.61, p=0.05, Nested one-way ANOVA; Veh vs. Ext p=0.02, Veh vs Rst 60 min p=0.331, Ext vs Rst 60 min, p=0.331, Holm-Sidak's multi-comparisons test). Also, correlations in cFos expression in D1-MSNs after 30 and 60 minutes Rst were run (Table S2 and S3) but not significant correlations were observed.

Discussion

Using THC+CBD SA we evaluated how daily exposure to two of the main constituents of cannabis affects glutamatergic transmission onto D1- and D2-MSNs in the NAcore. We found that the adaptations caused by THC+CBD were specific for D1 MSNs, distinct from adaptations described after heroin and cocaine use and only partially predicted the overall activity levels of these two cell types of MSNs in vehicle control, extinguished and reinstated animals.

Synaptic pruning decreased basal glutamate transmission in D1-MSNs but not D2-MSNs

Changes in spine morphology are a hallmark of drug-induced adaptations, with morphological potentiation produced following cocaine or nicotine self-administration[31–33], and depotentiation induced by opioids and THC[11,19,34] but see[35]. Similar to morphine[19], we expected a loss of dendritic spines selectively on D2-MSNs. Strikingly, we did not find that THC+CBD led to significant changes in overall spine density for neither cell type. However, the proportion of larger spines (0.45–0.60 μm head diameter) were reduced and spines with a head diameter smaller than 0.15 μm were increased in D1- but not on D2-MSNs. Since the density of AMPA receptors in the postsynapse is generally correlated with spine geometry, and small spines and filopodia only sparsely expressing AMPAR [36]. Thus, the increased number of small D1-MSN spines might not significantly contribute to AMPAR transmission. Indeed, the shift from large to small spines was accompanied by a loss of spontaneous events, hence we conclude that THC+CBD induced pruning of functional glutamatergic synapses onto D1-MSNs (Figure 2).

In D2-MSNs we found no spine changes after extinction from THC+CBD, but a small shift from larger to smaller spines after reinstatement, that was not reflected by changes in sEPSC amplitude or inter-event interval. This could indicate that the morphological depotentiation had no consequence for the basal glutamate transmission or that the recording of sEPSCs was not sufficiently sensitive to detect a change in a subset of synapses.

Specific desensitization of CB1R on glutamatergic synapses with D1-MSNs did not affect basal glutamate transmission but was paralleled by potentiated stimulated glutamate transmission.

We found reduced presynaptic inhibition of glutamate transmission after CB1R activation in brain tissue from animals that underwent extinction from THC+CBD SA as compared

to vehicle treated rats. This loss of CB1R function occurred specifically on glutamatergic afferents to NAc D1-MSNs. Since we did not detect a change in Paired-Pulse ratios, we conclude that this adaptation only affects glutamate transmission during increased network activity, as it might occur during cue-induced reinstatement. It would be interesting to test in future experiments whether positive allosteric modulators, which are able to partially rescue CB1R function[29] would inhibit cue-induced THC+CBD seeking.

CB1R dysfunction after THC+CBD was paralleled by LTP selectively in D1-MSNs after low frequency pairing stimulation, which could indicate that the CB1-dependent control of glutamate transmission is activity dependent. Akin to our previous publication we found that cue-induced reinstatement rectified D1-MSN associated metaplasticity after extinction from THC+CBD[9]. Cue-induced reinstatement causes a transient molecular reorganization at glutamatergic synapses in the NAc as well as associated astrocytes[37], hence many different molecular mechanisms, as for example changes in glutamate uptake, AMPAR subunit composition or changes in endocannabinoid signaling could be responsible for the rectification of plasticity. Future studies will investigate which of these changes will affect THC cue induced metaplasticity.

Change in cell type specific cFOS expression was only partially predicted by THC+CBD induced neuroadaptations

Neuroadaptations found during withdrawal from drugs of abuse often seem to counteract the acute drug effect and are often interpreted as homeostatic adaptations to balance acute drug-induced network perturbation[38]. However, a direct connection between cellular adaptations and changes in cellular activity has not often been established, leaving it unclear whether distinct neuroadaptations are homeostatic or driving drug induced activity changes that could contribute to relapse vulnerability. Here we compared the neuroadaptations identified after 10 days of chronic THC self-administration and changes in cFOS expression in D1 vs D2 MSNs. cFOS protein synthesis requires consistent high levels of Ca^{2+} influx, and therefore is commonly used as a proxy for neuronal activity[39]. We predicted that the loss of basal glutamate transmission in D1-MSNs after extinction from THC+CBD (Figure 2) would lead to decreased baseline activity but found that the percentage of D1 MSNs expressing cFOS remained unchanged 24h after the last extinction session. We conclude that the D1-MSN specific loss of functional synapses is not driving D1-MSN activity levels but is rather an allostatic response to acute THC+CBD induced network perturbations. Cue-induced cocaine seeking increases cFOS expression in D1-MSNs[40] and we also found a strong trend towards increased D1-MSN specific cFOS activity after 1h THC+CBD cue-induced reinstatement.

The percentage of D2 MSNS expressing cFOS was decreased 24h after the last extinction session which was partially restored after cue-induced reinstatement. Given that we could not find any adaptations in glutamate transmission that were associated with this D2-MSN hypoactivity or its rectification after reinstatement, we assume that the activity change is driven by changes upstream in the circuit or by changes in intrinsic excitability that we did not investigate in this study.

Limitations of this study and future directions:

Drug-induced vs. extinction-induced adaptations?—The animals in this study underwent extinction training in which they learn to dissociate drug context from drug availability. While this mode of drug withdrawal is a continuation of our previous studies and allows for isolation of the neurobiological effects of discrete drug-conditioned cues[22,29], it does not allow us to determine whether neuronal changes were caused by the chronic exposure to the drug, drug withdrawal, extinction training or a combination of all thereof. To distinguish between these possibilities, future studies need to compare adaptations at additional time points (for example 1day and 10 days after the last SA session) and abstinence (animals withdrawn outside of the drug-associated context). *Lack of plasticity in control animals*: Similar to our previous study in Sprague-Dawley rats we found differences in THC+CBD associated synaptic plasticity in the transgenic Long-Evans rats[9]. However, neither D1-MSNs nor D2-MSNs from drug naïve Cre rats expressed NMDAR-LTD, which is typically induced using this stimulus protocol. To test whether the lack of NMDAR-LTD was caused by the transgenes or reflects differences between the Sprague Dawley rats (used in previous publication) and Long Evans rats (background strain for D1- and D2-Cre rats), we conducted control experiments on untreated animals of both strains. Long Evans rats did not express LTD as compared to untreated Sprague-Dawley rats (Figure S6). Future studies will investigate whether strain-dependent differences in cannabinoid signaling caused these differences in plasticity thresholds between Long-Evans and Sprague-Dawley rats.

THC intravenous THC+CBD SA in comparison with other models of drug administration: The last decade has brought a diversification in murine models of drug abuse that aim to more accurately reflect different aspects of the abuse cycle[27,41,42]. Along with these innovations came a lot of polarization over which of these models have higher translational relevance. Non-contingent models of drug administration have provided most of the knowledge we have today about THC-induced neuronal adaptations[6,43,44] and will continue to be important. The availability of contingent THC SA models[22,45], now allows us to investigate i) neuroadaptations that depend on the behavioral contingency of drug delivery[46,47] and ii) neuroadaptations that arise during drug-seeking behavior[42]. The latter is particularly important because studies have shown that individuals recovering from cannabis use disorder have high relapse rates akin to other abused drugs[48]. Nevertheless, these SA models also have caveats: Training the animals is time-consuming and expensive, behavioral responses and thereby drug intake variable and the rewarding properties of THC+CBD lower as compared to other drugs of abuse. And while vapor self-administration models might more accurately reflect traditional routes of THC administration[45], the intravenous models allow to more precisely control drug intake and titrate drug concentrations. In summary we think that we will continue to need all of these models to advance our understanding of THC induced neuronal adaptations as well as the addictive potential of this drug.

Supplementary Material

Refer to Web version on PubMed Central for supplementary material.

Acknowledgments

This work was supported by National Institute on Drug Abuse Grant Nos. DA003906, DA012513, DA046373, and a VA Merit Award BX004727 (PWK), K99DA047426-01A1 (CGK), DA048337 and a NARSAD young investigator grant (DN). DN and PWK designed the research, DN, CG-K, MH, KS, VCC, LB, SS performed the research, DN and CG-K analyzed the data, and DN, CG-K and PWK wrote the article. We thank Eric Dereschewitz and Michael Scofield for technical assistance.

References

1. World Drug Report 2020; 2020. https://wdr.unodc.org/wdr2020/field/WDR20_Booklet_2.pdf
2. Hasin DS, Saha TD, Kerridge BT, et al. Prevalence of marijuana use disorders in the United States between 2001–2002 and 2012–2013. JAMA Psychiatry 2015;72(12):1235–1242. doi:10.1001/jamapsychiatry.2015.1858 [PubMed: 26502112]
3. Ferland J- MN, Hurd YL. Deconstructing the neurobiology of cannabis use disorder. Nat Neurosci Published online 2020. doi:10.1038/s41593-020-0611-0
4. Pertwee RG. The diverse CB 1 and CB 2 receptor pharmacology of three plant cannabinoids : D 9 -tetrahydrocannabinol, cannabidiol and D 9 -tetrahydrocannabivarin Published online 2008:199–215. doi:10.1038/sj.bjp.0707442
5. Chevaleyre V, Takahashi K a, Castillo PE. Endocannabinoid-mediated synaptic plasticity in the CNS. Annu Rev Neurosci 2006;29:37–76. doi:10.1146/annurev.neuro.29.051605.112834 [PubMed: 16776579]
6. Hoffman AF, Oz M, Caulder T, Lupica CR. Functional tolerance and blockade of long-term depression at synapses in the nucleus accumbens after chronic cannabinoid exposure. J Neurosci 2003;23(12):4815–4820. doi:23/12/4815 [pii] [PubMed: 12832502]
7. Mato S, Robbe D, Puente N, Grandes P, Manzoni OJ. Presynaptic homeostatic plasticity rescues long-term depression after chronic Delta 9-tetrahydrocannabinol exposure. J Neurosci 2005;25(50):11619–11627. doi:10.1523/JNEUROSCI.2294-05.2005 [PubMed: 16354920]
8. Lazenka MF, Selley DE, Sim-Selley LJ. dFosB induction correlates inversely with CB 1 receptor desensitization in a brain region-dependent manner following repeated D 9 -THC administration. Neuropharmacology 2014;77:224–233. doi:10.1016/j.neuropharm.2013.09.019 [PubMed: 24090766]
9. Neuhofer D, Spencer SM, Chioma VC, Beloate LN, Schwartz D, Kalivas PW. The loss of NMDAR-dependent LTD following cannabinoid self-administration is restored by positive allosteric modulation of CB1 receptors. Addict Biol 2020;25(6):1–10. doi:10.1111/adb.12843
10. Miller ML, Chadwick B, Dickstein DL, et al. Adolescent exposure to Δ9-tetrahydrocannabinol alters the transcriptional trajectory and dendritic architecture of prefrontal pyramidal neurons. Mol Psychiatry Published online 2018. doi:10.1038/s41380-018-0243-x
11. Spencer S, Neuhofer D, Chioma VC, et al. A Model of Δ9-Tetrahydrocannabinol Self-administration and Reinstatement That Alters Synaptic Plasticity in Nucleus Accumbens. Biol Psychiatry 2018;84(8):601–610. doi:10.1016/j.biopsych.2018.04.016 [PubMed: 29861097]
12. Floresco SB. The Nucleus Accumbens: An Interface Between Cognition, Emotion, and Action. Annu Rev Psychol 2015;66(1):25–52. doi:10.1146/annurev-psych-010213-115159 [PubMed: 25251489]
13. Neuhofer D, Kalivas P. Metaplasticity at the addicted tetrapartite synapse: A common denominator of drug induced adaptations and potential treatment target for addiction. Neurobiol Learn Mem 2018;154. doi:10.1016/j.nlm.2018.02.007
14. Kalivas PW. The glutamate homeostasis hypothesis of addiction. Nat Rev Neurosci 2009;10(8):561–572. doi:10.1038/nrn2515 [PubMed: 19571793]
15. Smith RJ, Lobo MK, Spencer S, Kalivas PW. Cocaine-induced adaptations in D1 and D2 accumbens projection neurons (a dichotomy not necessarily synonymous with direct and indirect pathways). Curr Opin Neurobiol 2013;23(4):546–552. doi:10.1016/j.conb.2013.01.026 [PubMed: 23428656]

16. Calipari ES, Bagot RC, Purushothaman I, et al. In vivo imaging identifies temporal signature of D1 and D2 medium spiny neurons in cocaine reward. Proc Natl Acad Sci U S A 2016;113(10):2726–2731. doi:10.1073/pnas.1521238113 [PubMed: 26831103]

17. Heinsbroek JA, Neuhofer D, Griffin WC, et al. Loss of Plasticity in the D2-Accumbens Pallidal Pathway Promotes Cocaine Seeking. J Neurosci 2017;37(4):757–767. doi:10.1523/JNEUROSCI.2659-16.2016 [PubMed: 28123013]

18. Pascoli V, Terrier J, Espallergues J, Valjent E, O'Connor EC, Lüscher C. Contrasting forms of cocaine-evoked plasticity control components of relapse. Nature 2014;509(7501):459–464. doi:10.1038/nature13257 [PubMed: 24848058]

19. Graziane NM, Sun S, Wright WJ, et al. Opposing mechanisms mediate morphine- and cocaine-induced generation of silent synapses. Nat Neurosci 2016;19(7):915–925. doi:10.1038/nn.4313 [PubMed: 27239940]

20. Roberts-Wolfe D, Bobadilla A-C, Heinsbroek JA, Neuhofer D, Kalivas PW. Drug Refraining and Seeking Potentiate Synapses on Distinct Populations of Accumbens Medium Spiny Neurons. J Neurosci 2018;38(32):7100–7107. doi:10.1523/jneurosci.0791-18.2018 [PubMed: 29976626]

21. Klein C, Karanges E, Spiro A, et al. Cannabidiol potentiates Δ9-tetrahydrocannabinol (THC) behavioural effects and alters THC pharmacokinetics during acute and chronic treatment in adolescent rats. Psychopharmacology (Berl) 2011;218(2):443–457. doi:10.1007/s00213-011-2342-0 [PubMed: 21667074]

22. Spencer S, Neuhofer D, Chioma VC, et al. A Model of Δ^9-Tetrahydrocannabinol Self-administration and Reinstatement That Alters Synaptic Plasticity in Nucleus Accumbens. Biol Psychiatry 2018;84(8). doi:10.1016/j.biopsych.2018.04.016

23. Pardo-Garcia TR, Garcia-Keller C, Penaloza T, et al. Ventral Pallidum Is the Primary Target for Accumbens D1 Projections Driving Cocaine Seeking. J Neurosci 2019;39(11):2041–2051. doi:10.1523/JNEUROSCI.2822-18.2018 [PubMed: 30622165]

24. Gipson CD, Kupchik YM, Shen H-W, Reissner KJ, Thomas C a, Kalivas PW. Relapse induced by cues predicting cocaine depends on rapid, transient synaptic potentiation. Neuron 2013;77(5):867–872. doi:10.1016/j.neuron.2013.01.005 [PubMed: 23473317]

25. Barros VN, Mundim M, Galindo LT, Bittencourt S, Porcionatto M, Mello LE. The pattern of c-Fos expression and its refractory period in the brain of rats and monkeys. Front Cell Neurosci 2015;9(March):1–8. doi:10.3389/fncel.2015.00072 [PubMed: 25667569]

26. Martin M, Chen BT, Hopf FW, Bowers MS, Bonci A. Cocaine self-administration selectively abolishes LTD in the core of the nucleus accumbens. Nat Neurosci 2006;9(7):868–869. doi:10.1038/nn1713 [PubMed: 16732275]

27. Kasanetz F, Deroche-Gamonet V, Berson N, et al. Transition to addiction is associated with a persistent impairment in synaptic plasticity. Science (80-) 2010;328(5986):1709–1712. doi:10.1126/science.1187801

28. Viswanathan S, Williams ME, Bloss EB, et al. High-performance probes for light and electron microscopy. 2015;12(6):568–576.

29. Neuhofer D, Spencer SM, Chioma VC, Beloate LN, Schwartz D, Kalivas PW. The loss of NMDAR-dependent LTD following cannabinoid self-administration is restored by positive allosteric modulation of CB1 receptors. Addict Biol 2020;25(6). doi:10.1111/adb.12843

30. Johnson AR, Thibeault KC, Lopez AJ, et al. Cues play a critical role in estrous cycle-dependent enhancement of cocaine reinforcement. Neuropsychopharmacology 2019;(January). doi:10.1038/s41386-019-0320-0

31. Gipson CD, Kupchik YM, Shen H-W, Reissner KJ, Thomas A, Kalivas PW. NIH Public Access 2014;77(5):867–872. doi:10.1016/j.neuron.2013.01.005.Relapse

32. Garcia-Keller C, Neuhofer D, Bobadilla A-C, et al. Extracellular Matrix Signaling Through β3 Integrin Mediates Cocaine Cue-induced Transient Synaptic Plasticity and Relapse. Biol Psychiatry 2019;(6):1–11. doi:10.1016/j.biopsych.2019.03.982

33. Gipson CD, Reissner KJ, Kupchik YM, et al. Reinstatement of nicotine seeking is mediated by glutamatergic plasticity. Proc Natl Acad Sci U S A 2013;110(22):9124–0120. doi:10.1073 [PubMed: 23671067]

34. Shen H-W, Moussawi K, Zhou W, Toda S, Kalivas PW. Heroin relapse requires long-term potentiation-like plasticity mediated by NMDA2b-containing receptors. Proc Natl Acad Sci U S A 2011;108(48):19407–19412. doi:10.1073/pnas.1112052108 [PubMed: 22084102]
35. Chioma VC, Kruyer A, Bobadilla AC, et al. Heroin Seeking and Extinction From Seeking Activate Matrix Metalloproteinases at Synapses on Distinct Subpopulations of Accumbens Cells. Biol Psychiatry 2021;89(10):947–958. doi:10.1016/j.biopsych.2020.12.004 [PubMed: 33579535]
36. Matsuzaki M, Ellis-Davies GCR, Nemoto T, Miyashita Y, Iino M, Kasai H. Dendritic spine geometry is critical for AMPA receptor expression in hippocampal CA1 pyramidal neurons. Nat Neurosci 2001;4(11):1086–1092. doi:10.1038/nn736 [PubMed: 11687814]
37. Kruyer A, Kalivas PW. Astrocytes as cellular mediators of cue reactivity in addiction. Curr Opin Pharmacol 2021;56:1–6. doi:10.1016/j.coph.2020.07.009 [PubMed: 32862045]
38. Muntean BS, Dao MT, Martemyanov KA, Muntean BS, Dao MT, Martemyanov KA. Allostatic Changes in the cAMP System Drive Opioid-Induced Adaptation in Striatal Dopamine Signaling Article Allostatic Changes in the cAMP System Drive Opioid-Induced Adaptation in Striatal Dopamine Signaling. CellReports 2019;29(4):946–960.e2. doi:10.1016/j.celrep.2019.09.034
39. Cruz FC, Koya E, Guez-Barber DH, et al. New technologies for examining the role of neuronal ensembles in drug addiction and fear. Nat Rev Neurosci 2013;14(11):743–754. doi:10.1038/nrn3597 [PubMed: 24088811]
40. Bobadilla AC, Dereschewitz E, Vaccaro L, Heinsbroek JA, Scofield MD, Kalivas PW. Cocaine and sucrose rewards recruit different seeking ensembles in the nucleus accumbens core. Mol Psychiatry 2020;25(12):3150–3163. doi:10.1038/s41380-020-00888-z [PubMed: 32985600]
41. Venniro M, Zhang M, Caprioli D, et al. Volitional social interaction prevents drug addiction in rat models. Nat Neurosci 2018;21(11):1520–1529. doi:10.1038/s41593-018-0246-6 [PubMed: 30323276]
42. Kuhn BN, Kalivas PW, Bobadilla AC. Understanding Addiction Using Animal Models. Front Behav Neurosci 2019;13(November):1–24. doi:10.3389/fnbeh.2019.00262 [PubMed: 30697155]
43. Hwang EK, Lupica CR. Altered Corticolimbic Control of the Nucleus Accumbens by Long-term Δ9-Tetrahydrocannabinol Exposure. Biol Psychiatry Published online 2019:1–13. doi:10.1016/j.biopsych.2019.07.024
44. Mato S Presynaptic Homeostatic Plasticity Rescues Long-Term Depression after Chronic 9-Tetrahydrocannabinol Exposure. J Neurosci 2005;25(50):11619–11627. doi:10.1523/JNEUROSCI.2294-05.2005 [PubMed: 16354920]
45. Freels TG, Baxter-Potter LN, Lugo JM, et al. Vaporized cannabis extracts have reinforcing properties and support conditioned drug-seeking behavior in rats. J Neurosci 2020;40(9):1897–1908. doi:10.1523/JNEUROSCI.2416-19.2020 [PubMed: 31953372]
46. Lecca D, Cacciapaglia F, Valentini V, Acquas E, Di Chiara G. Differential neurochemical and behavioral adaptation to cocaine after response contingent and noncontingent exposure in the rat. Psychopharmacology (Berl) 2007;191(3):653–667. doi:10.1007/s00213-006-0496-y [PubMed: 16932924]
47. Lominac KD, Sacramento AD, Szumlinski KK, Kippin TE. Distinct neurochemical adaptations within the nucleus accumbens produced by a history of self-administered vs non-contingently administered intravenous methamphetamine. Neuropsychopharmacology 2012;37(3):707–722. doi:10.1038/npp.2011.248 [PubMed: 22030712]
48. . Moore BA, Budney AJ. Relapse in outpatient treatment for marijuana dependence. J Subst Abuse Treat 2003;25(2):85–89. doi:10.1016/S0740-5472(03)00083-7 [PubMed: 14629990]

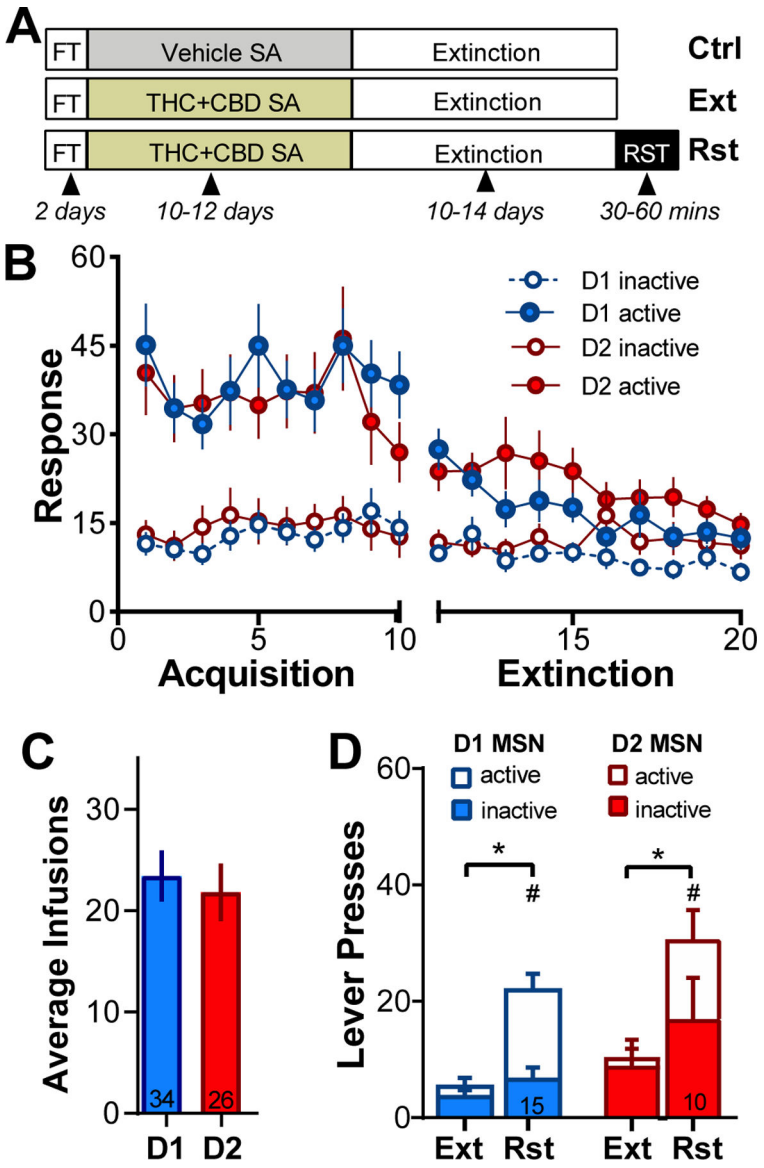

Figure 1. Treatment groups and THC+CBD SA behavior.

A) Timeline. 3 different treatment groups, vehicle control (Ctrl), extinguished (Ext), reinstated (Rst) were tested. **B)** Comparable THC+CBD SA and extinction of D1 vs D2 Cre lines (left panel) and female vs male (right panel). 2-way ANOVA revealed no significant difference in active lever presses between strains or sex. **C)** The average daily infusion rates over the last 5 days of SA revealed no difference in intake between D1 vs D2 Cre rats **D)** Active and inactive lever pressing during 30 min of cued-reinstatement compared to average lever pressing of the last 3 days of extinction training. *p<0.05 (comparison Rst vs Ext), #p<0.05 (comparison active vs inactive).

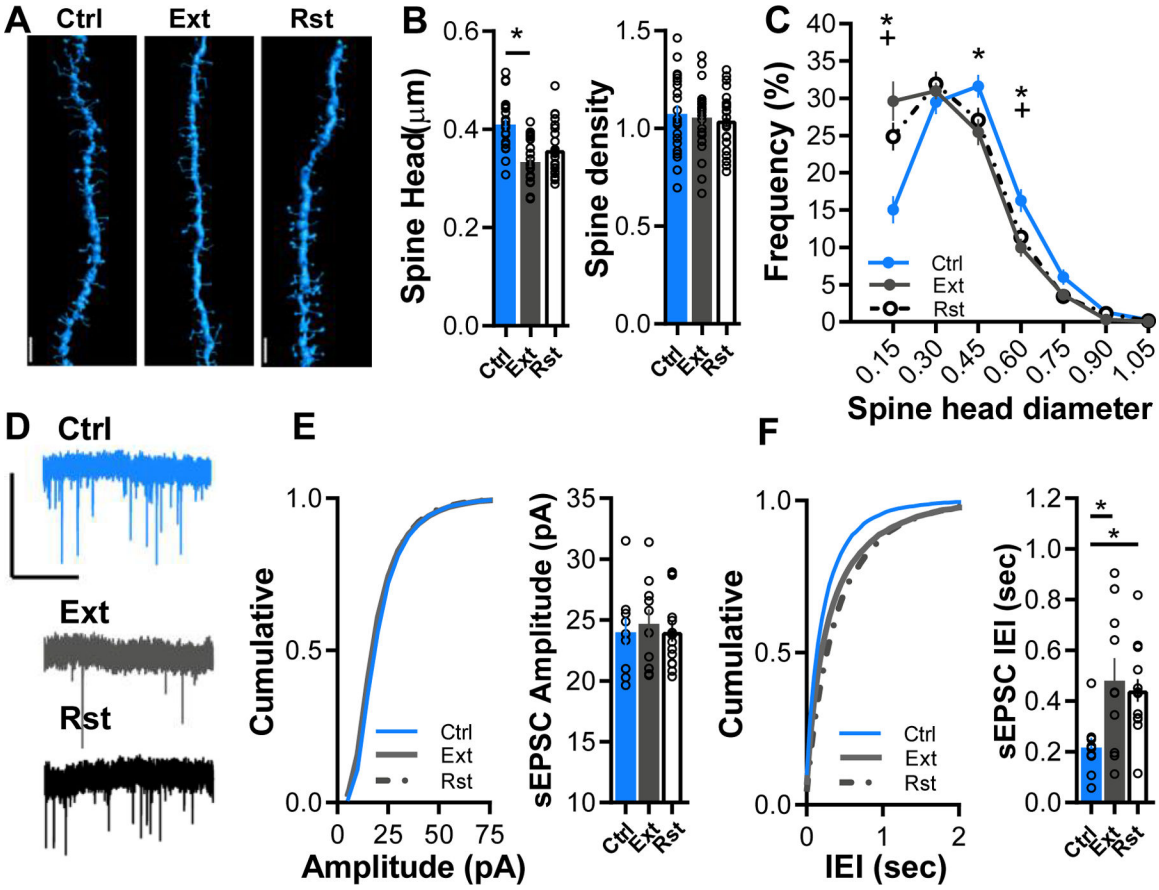

Figure 2. Extinction from THC+CBD SA induces a loss of large spines and reduces spontaneous glutamatergic transmission in D1 Medium Spiny Neurons.

A) Representative dendritic segment from NAcore D1-MSNs for each treatment group. Bar=5 μm. **B)** left bar chart: Significant reduction dendritic spine head diameter between vehicle (Veh) and THC+CBD extinguished rats. Right bar chart: No significant change in overall spine density between treatment groups. **C)** Frequency distribution of Spine head sizes reveals significant changes in spine density between treatment groups that are dependent on spine head diameter. *p<0.05 comparing Ctrl vs. Ext; $^{+}$p=<0.05 comparing Ctrl. Vs. Rst **D)** Representative traces of spontaneous activity from NAcore D1-MSNs for each treatment group. Scale bar shows 50pA vs 2 sec. **E)** Cumulative probability and mean values of amplitude for sEPSCs indicate no difference between treatment groups. **F)** Cumulative probability and mean values of sEPSC interevent-intervals from D1-MSNs show a reduction in spontaneous glutamate transmission in THC+CBD extinguished and cue-reinstated rats. (p=0.04, Kruskal-Wallis test with Dunn's multiple comparison). All data are shown as mean ± SEM; *p<0.05. **A-C)** N is shown as number of neurons quantified over number of animals in each condition (neurons/animals): vehicle N=21/5; THC+CBD extinguished N=24/5; reinstated N=23/5. **D-F)** N is shown as number of neurons quantified over number of animals in each condition (cells/animals): vehicle N=9/5; THC+CBD extinguished N=10/6; THC+CBD reinstated N=14/7).

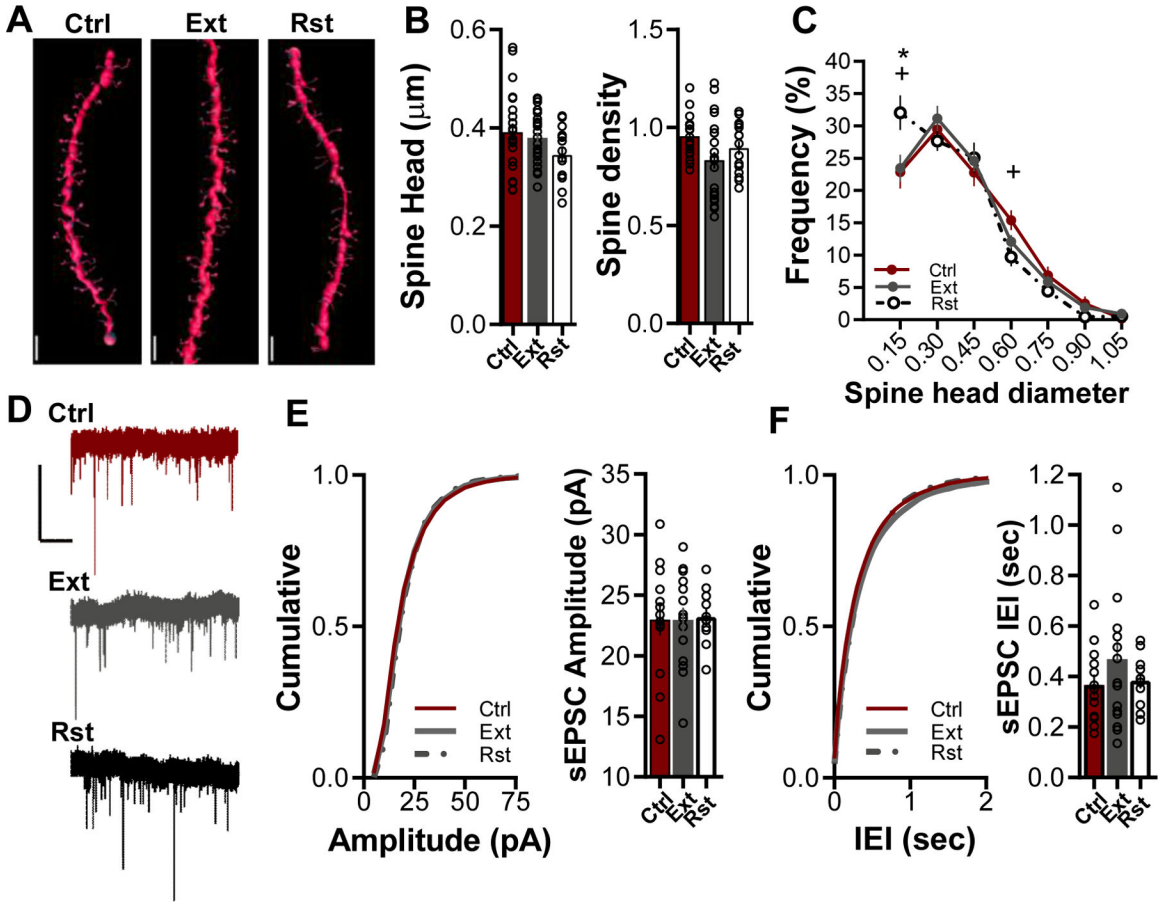

Figure 3. Cued-Reinstatement induces a pruning of large spines but does not affect spontaneous glutamatergic transmission in D2 Medium Spiny Neurons.

A) Representative dendrites from NAcore D2-MSNs for each treatment group. Bar=5 μm. **B)** There was no significant change in spine head diameter (left bar chart) or spine density (right bar chart) **C)** Frequency distribution reveals spine head dependent changes in spine density between treatment groups. *p<0.05 comparing Ctrl vs. Ext; $^{+}$p=<0.05 comparing Ctrl. Vs. Rst. **D)** Representative traces of spontaneous activity from NAcore D2-MSNs for each treatment group. Scale bar shows 50 pA vs 2 sec. **E)** Cumulative probability and mean values of amplitude for sEPSCs recordings from D2-MSNs show no difference between treatment groups. **F)** Cumulative probability and mean values of sEPSC Inter-Event-Intervals show no difference between treatment groups. All data are shown as mean ± SEM. *p<0.05. **A-C)** N is shown as number of neurons quantified over number of animals in each condition (neurons/animals): vehicle N=22/4; THC+CBD extinguished N=23/4; THC+CBD reinstated N:15/3. **D-F)** N is shown as number of neurons quantified over number of animals in each condition (neurons/animals): vehicle N=13/8; THC+CBD extinguished N=15/7; Reinstated N=11/5.

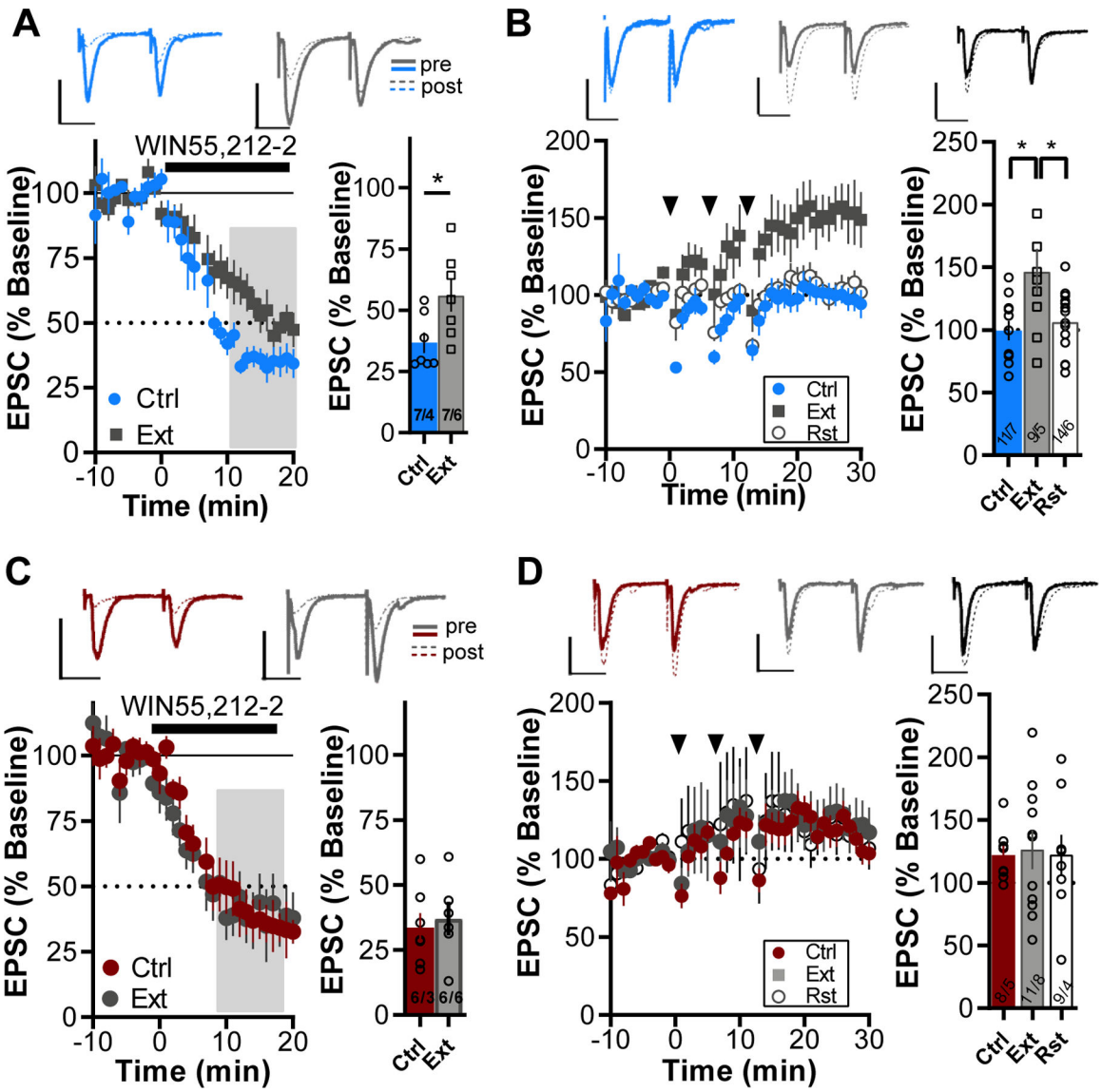

Figure 4. Extinction from THC+CBD SA impedes CB1R function and induces long-term potentiation of glutamate transmission in D1 but not D2 Medium Spiny Neurons.

A) (Top) Representative D1 MSN current traces pre and post WIN55,212–2 application from a vehicle and a THC+CBD extinguished rat. Scale bar: 550 pA vs 25 ms. Left: Averaged EPSC shows that WIN55,212–2 (5 μM) reduced EPSC amplitude to a larger extend in vehicle rats that in D1 MSNs of THC-CBD extinguished. Right: Bar graph summarizing the average response 15 to 25 minutes into WIN55,2121–2 application. N is shown as number of cells quantified over number of animals in each condition (cells/animals): vehicle N=7/4; THC+CBD extinguished N=7/6. *p<0.05 comparing baseline response to 10–20 min after WIN application. **B)** (Top) Representative D1 MSN current traces pre and post plasticity induction. Left: Time course of D1 MSNs synaptic response to the induction protocol. Extinction of THC + CBD induced metaplasticity that was rectified by 30 minutes of cue-induced. Right: Bar graph summarizing the average response 15 to 25 minutes after LTD induction. D1-MSNs in slices of THC extinguished animals

exhibited significant LTP but not reinstated or control animals exhibited significant LTP. *p<0.05 comparing baseline response to 15 to 25 post-induction. N is shown as number of cells quantified over number of animals in each condition (cells/animals): vehicle N=11/7; THC+CBD extinguished N=9/5; THC+CBD reinstated N=14/6). **C)** (Top) Sample D2 MSN current traces pre and post WIN55,212–2 application from the three treatment groups. Scale bar: 550pA vs 25 ms. Left: Average time course of CB1 agonist WIN55,212–2 dependent inhibition of EPSPs revealed no difference between treatment groups. Right: Bar graph summarizing the average response 15 to 25 minutes into WIN55,2121–2. N is shown as number of cells quantified over number of animals in each condition (cells/animals): vehicle N=6/3; THC+CBD extinguished N=6/6. **D)** (Top) Representative current traces pre and post plasticity induction. Left: Time course of D2-MSNs synaptic response to plasticity induction protocol revealed no difference between treatment groups. Right: Bar graph show averaged responses, comparing baseline to the average of 15–25 min after LTD induction protocol. N is shown as number of cells quantified over number of animals in each condition (cells/animals): vehicle N=8/5; THC+CBD extinguished N=11/8; THC+CBD reinstated N=9/4). *p<0.05, *comparing treatment groups.

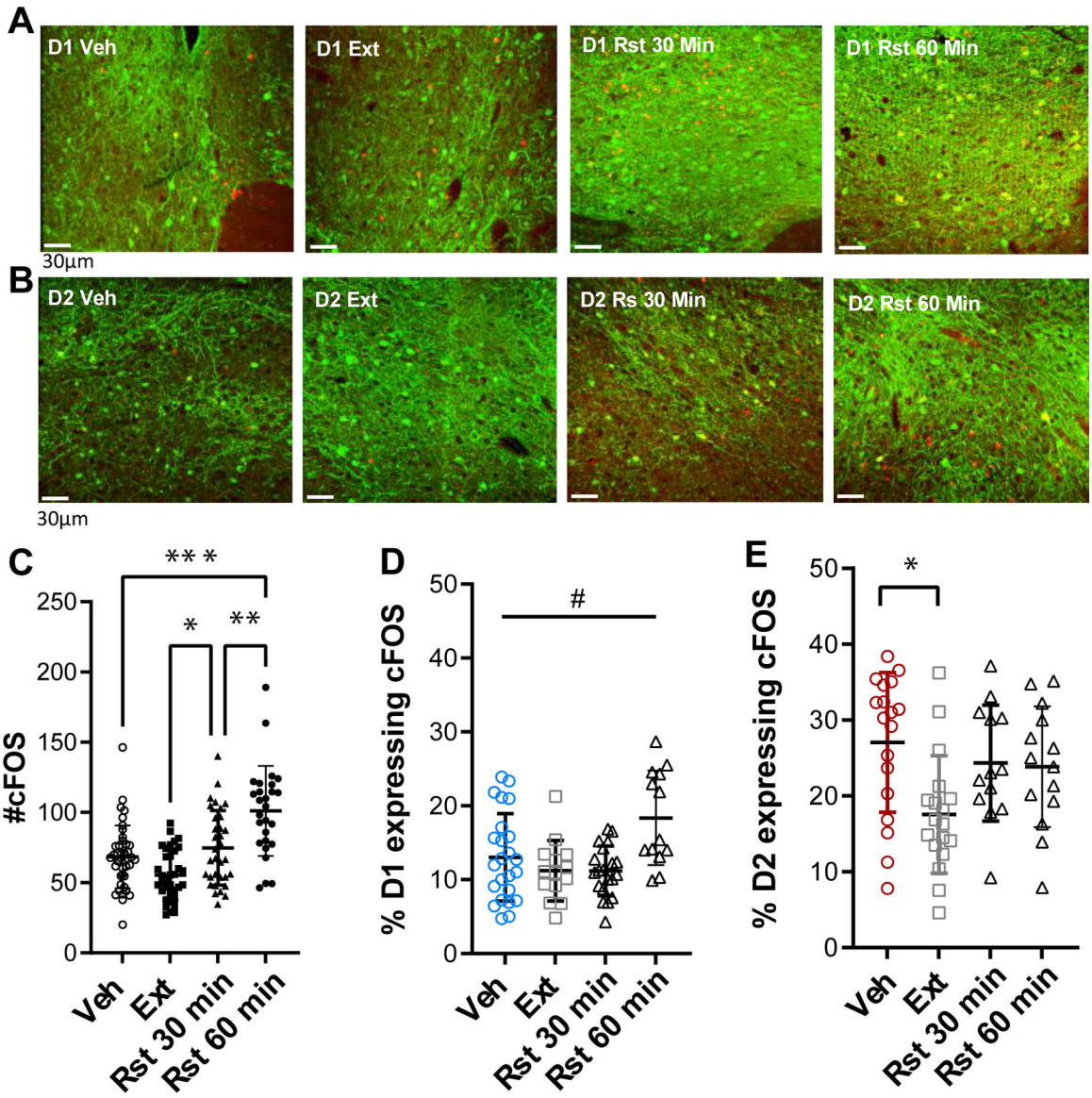

Figure 5. Cell type specific effects of Extinction from THC+CBD and cue-induced reinstatement on cFOS expression.

A) Representative images of cFOS (red) and D1 MSNs (green) labeling in the nucleus accumbens core in a vehicle (D1 Veh), THC+CBD extinduished (D1 Ext) and cue-reinstated (D1 Rst) rat. Scale bar = 20µm. **B)** Representative images of cFOS (red) and D2 MSNs (green) labeling in the nucleus accumbens core in a vehicle (D2 Veh), THC+CBD extinduished (D2 Ext) and cue-reinstated (D2 Rst). **C)** Scatter dot plot illustrating the significant increase in cFOS expression after cue-induced reinstatement to THC. **D)** The percentage of D1 expressing c-FOS cells was significantly modulated by the behavioral state. $^{\#}p<0.05$ Nested-One way ANOVA but no significant Holm-Sidak's multiple comparisons post hoc. N is shown as number of pictures quantified over number of animals in each condition (pictures/animals): vehicle N=24/6; THC+CBD extinguished N=14/3; THC+CBD 30 min reinstated N=20/5; THC+CBD 60 min reinstated N=13/3). **E)** Extinction from THC+CBD decreased the overall activity of D2 MSNS which was rectified

after cue-induced reinstatement. N is shown as number of pics quantified over number of animals in each condition (pictures/animals): vehicle N=18/4; THC+CBD extinguished N=18/4; THC+CBD 30 min reinstated N=13/3; THC+CBD 60 min reinstated N=14/3).